

Changing the order of a dynamical phase transition through fluctuations in a quantum p -spin model.

Lorenzo Correale^{1,2} and Alessandro Silva¹

¹*SISSA — International School for Advanced Studies, via Bonomea 265, I-34136 Trieste, Italy*

²*INFN — Istituto Nazionale di Fisica Nucleare, Sezione di Trieste, I-34136 Trieste, Italy*

(Dated: October 27, 2021)

We study the non-equilibrium phase diagram of a fully-connected Ising p -spin model, for generic $p > 2$, and investigate its robustness with respect to the inclusion of spin-wave fluctuations, described by a ferromagnetic, short-range spin interaction. We investigate the dynamics of the mean-field model after a quantum quench observing a new dynamical quantum phase transition which is either first or second order depending on the even or odd parity of p , in stark contrast with the static first order counterpart for all p . In addition, we find that the corresponding phase diagram is qualitatively modified by the fluctuations introduced by a short-range interaction which drive the system always towards various paramagnetic phases distinguished by the strength of time dependent fluctuations of the magnetization.

PACS numbers: 05.30.Rt, 64.60.Ht, 75.10.Jm

Equilibrium phase transition, either at zero or finite-temperature, are known to leave a substantial imprint in the nonequilibrium dynamics of a quantum many-body system [1]. For example, even when a stationary state attained after a quantum quench does not reveal signatures of order as in low-dimensional systems [2–4], a linear ramp through a second order quantum critical point leaves universal signatures in the scaling of the number of excitations with the ramp speed [5–8], as confirmed extensively in a number of experiments [9–15]. Analogous signatures are left when a first order quantum phase transition is crossed [16–18] through the nucleation of resonant bubbles of the new phase close to the critical point [19–21] which leads to a modified Kibble-Zurek-like power-law scaling [22].

Among the signatures of criticality observed out-of-equilibrium, dynamical critical phenomena occupy a special place. Dynamical criticality can be observed as singular temporal behavior of the Loschmidt echo (LE) most notably when a quench across a quantum phase transition is performed [23–25], even in situations where long-range order cannot be sustained in stationary states. In systems with long-range interactions, on the contrary, intertwined with the singular behavior of the LE [26], a standard Landau-type critical behavior based on the dependence of the time averaged order parameter with respect to the quench parameters can be observed [27, 28]. Peculiar to these second-order dynamical transitions is the fact that they are associated to critical trajectories with a divergent time scale in the dynamics separating revivals with a finite order parameter [26, 29]. In the presence of fluctuations critical trajectories become unstable and second order dynamical critical points widen up into chaotic dynamical phases [30–33].

While a great deal is known about second-order dynamical phase transitions, the dynamics of first order transitions is much less explored. The notion of dynamical

criticality associated to the LE has been extended to include first order behavior [34] while first-order and dissipative phase transitions in infinite range p -spin systems coupled to an external bath have been studied in Ref.[35]. In this work we address dynamical phase transitions and their stability against fluctuations in a system displaying a first order equilibrium transition: a spin system with infinite range p -spin interactions in transverse field. We show that, already at mean-field level, the system undergoes a DQPT, driven by a transverse field g , whose order depends non-trivially on p , despite its equilibrium counterpart being always of first order. We then perturb it by a short-range two-body interaction tuning the strength of spin fluctuations [30, 31]. While for $p = 2$ a chaotic dynamical region opens up near the mean-field criticality [30, 31], we show that for $p > 2$ dynamical chaos is almost entirely replaced by a new dynamical paramagnetic region, which appears above some threshold of the short-ranged coupling. We show that this is due to the emission of energy in the form of spin-waves, which predominantly drive the system into a paramagnetic minimum even in the presence of other minima in the energy landscape.

Our starting point is going to be the study of the dynamics of N spins $1/2$ subject to all-to-all p -body and a global transverse field g [36, 37]. Its Hamiltonian is defined as

$$\hat{H}_0 = -\frac{\lambda}{N^{p-1}} \sum_{i_1 \dots i_p=1}^N \hat{\sigma}_{i_1}^x \dots \hat{\sigma}_{i_p}^x - g \sum_i \hat{\sigma}_i^z \quad (1)$$

where $\hat{\sigma}_i^\alpha$ are the Pauli matrices at site i . The fully connected p -spin model, which was originally introduced in the context of spin-glasses [36, 37], plays a central role for studies on quantum annealing [38, 39]: its zero-temperature phase diagram can be derived analytically [38–40] and displays a quantum phase transitions driven

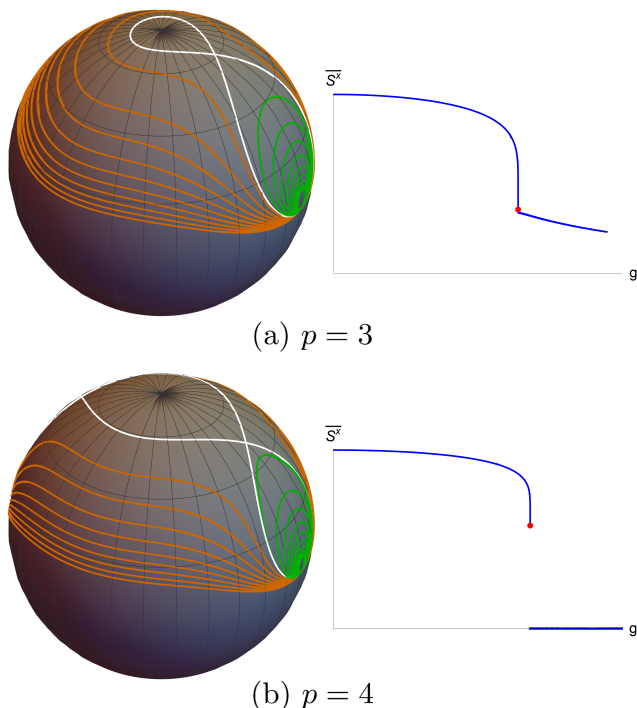


FIG. 1. From left to right, we plot the trajectories of the magnetization $\vec{S}(t)$ and the corresponding time-averaged magnetization \bar{S}^x , described after a quench starting in $S^x(0) = 1$, as functions of the post-quench values of g , for the two cases of (a) $p = 3$ and (b) $p = 4$. **(Left)** For both values of p , the system evolves on trajectories which either are confined in a ferromagnetic well (green), for $g < g_{dyn}$, or enclose all the local minima (orange), for $g > g_{dyn}$. The two regions are separated by a critical trajectory (white), corresponding to $g = g_{dyn}$. **(Right)** Plot of the dynamical order parameter \bar{S}^x as a function of g . At the critical point (red dot), this is continuous for $p = 3$ only.

by g , continuous for $p = 2$ and of the first-order for $p > 2$. In the following we will first address its dynamics and dynamical phase transitions. We will then study the effect of fluctuations by adding to the Hamiltonian a nearest-neighbour interaction term, in the spirit of Ref.30, written in the momentum space as

$$\hat{U} = -J \sum_{k \neq 0} \cos k \tilde{\sigma}_k^x \tilde{\sigma}_{-k}^x \quad (2)$$

with k being integer multiple of $2\pi/N$ and N is the system size. The first observation that we make is that the order of a DQPT does not necessarily follow that of the equilibrium transition. The case $p = 2$ is special, as it displays both second order equilibrium as well as a dynamical phase transitions [27, 29]. For $p > 2$ the equilibrium phase transition becomes instead first order: the energy landscape obtained from the mean-field Hamiltonian Eq.(1) is not simply double-well shaped and displays a paramagnetic local minimum at $S^x = 0$, together with one positive ferromagnetic minimum for $p \geq 3$ odd or two

opposite ferromagnetic minima for $p \geq 4$ even. For the two cases we report results obtained in the paradigmatic examples of $p = 3$ and $p = 4$, respectively.

The different interplay between various stationary points is expected to change qualitatively the nature of the DQPT, both in the mean-field limit and in presence of short-range interaction at $J \neq 0$, which are taken into account via a time-dependent spin-wave analysis [30, 41]. In order to show this we start by analyzing the dynamics resulting from Eq. 1 in the mean-field large N limit. Starting from a ferromagnetic initial condition $\langle S^x \rangle = 1$ we integrate the mean-field equations numerically for a range of post-quench values of the transverse field g and for each of them we compute the classical trajectory described by $\vec{S}(t)$ on the Bloch sphere and the dynamical order parameter $\bar{S}^x = \lim_{T \rightarrow \infty} \int_0^T S^x(t)/T$. The results, summarized Fig. 1, show the emergence of a DQPT whose qualitative features depend on the parity of p , unlike its static counterpart. For $p \geq 3$ odd, the transition is continuous as in the case of $p = 2$. The origin of this continuity lies in the symmetry of the dynamical trajectories on the Bloch sphere: while for $g < g_c$ trajectories are confined close to the ferromagnetic minimum (green trajectories, Fig.1-(a)), for $g > g_c$ they encircle both minima (orange trajectories, Fig.1-(a)), ferromagnetic and paramagnetic, effectively leading to a weighted average of the longitudinal magnetization that is continuous at g_c . The situation changes, because of symmetry, for $p \geq 4$ even: while approaching the critical point from below, where the dynamics is confined in the rightmost ferromagnetic sector, \bar{S}^x still tends to a nonvanishing local maximum (green trajectories, Fig.1-(b)), it vanishes abruptly when we move even slightly above the transition point because trajectories are this time symmetric with respect to the $y - z$ plane (orange trajectories, Fig.1-(b)).

The change of the order of the phase transition at mean-field level as the system is driven out of equilibrium is an effect that may be further enhanced by the presence of fluctuations that for $p = 2$ may even melt a dynamical critical point into an entire chaotic region of the phase diagram. To understand this phenomenon, we follow Ref. [30] and consider the quench dynamics of the p -spin model under the influence of an extra term of the Hamiltonian (Eq. (2)). We treat the resulting spin-wave fluctuations as a small perturbation to the dynamics of the classical collective spin $\vec{S}(t)$: we first rewrite the spin operators Eq.(1) in a time-dependent reference frame $\mathcal{R} = (\mathbf{X}, \mathbf{Y}, \mathbf{Z})$, implemented via the unitary rotation $V(\theta(t), \phi(t)) = \exp(-i\phi(t) \sum_i \sigma_i^z / 2) \exp(-i\theta(t) \sum_i \sigma_i^y / 2)$, where the spherical angles $\theta(t)$ and $\phi(t)$ are fixed in such a way that the magnetization $\vec{S}(t)$ is aligned with the Z -axis in the new frame, for any $t > 0$. Furthermore, assuming that the fluctuations, transverse to $\mathbf{Z}(t)$, are small, we expand the spin variables in the new frame through the

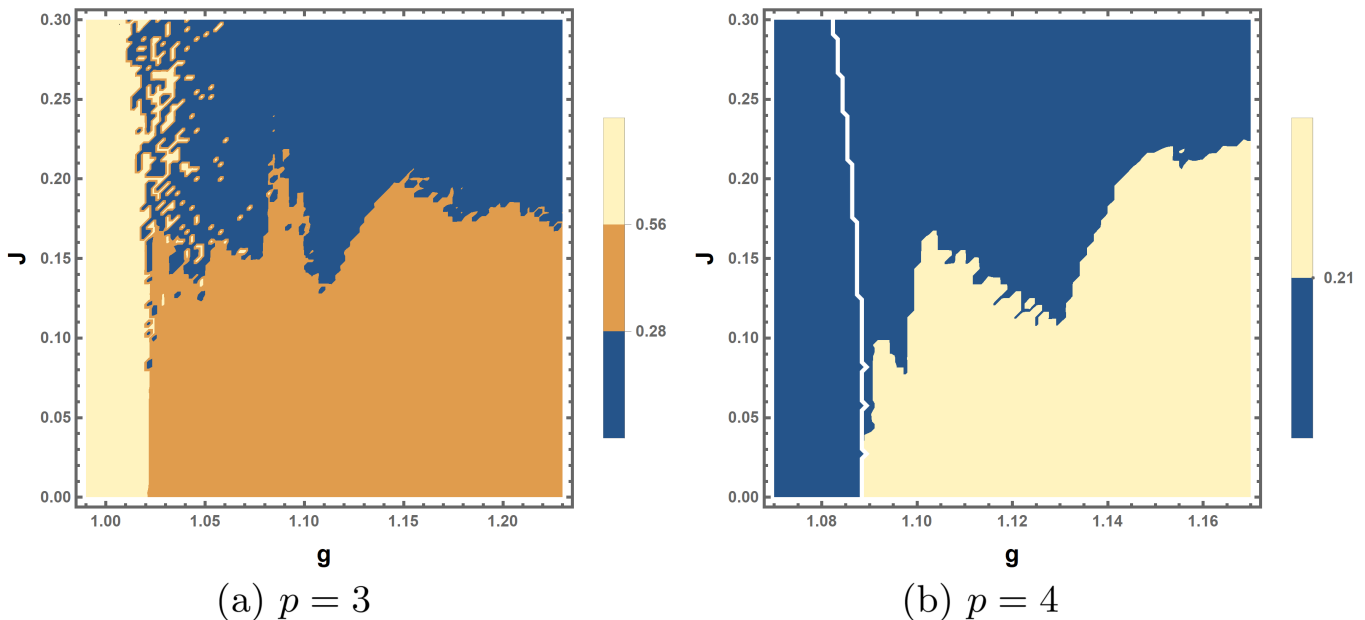


FIG. 2. Non-equilibrium phase diagram of the p -spin model Eq.(1), obtained integrating equations Eq.(4) for a quench starting from the fully polarized state $S^x(0) = 1$ and for a system size $N = 100$. We set $\lambda = 1$. (a) Phase diagram representing the time-averaged magnetization $\overline{S^x}$ for $p = 3$, as a function of the post-quench values of g and J . The dynamical ferromagnetic (beige) and dynamical bi-stable phase (orange) are the same we found in the mean-field limit (Fig. 1). The latter is replaced by a dynamical paramagnetic phase (blue) for sufficiently large J , with the magnetization localizing in the well around $S^z = 1$, while a narrow chaotic region can be observed around the mean-field criticality. (b) Time-averaged fluctuations $(\overline{\delta S^x})^2$, for $p = 4$. Two main regions can be identified in the diagram: a localized one (blue), where $S^x(t)$ is confined in one of the wells of the energy landscape, and a paramagnetic one (beige), where it performs wide oscillations around all the three minima. The first one coincides either with the dynamical ferromagnetic phase (if $g < g_{dyn}$), or with a localized paramagnetic phase (if $g > g_{dyn}$). The two are separated by white transition line, which marks the border of the dynamical paramagnetic region (see also Section 2 of Supplementary Material for further details).

Holstein–Primakoff (HP) transformation [42]

$$\begin{aligned} \hat{\sigma}_i^X &\simeq \hat{q}_i/\sqrt{s}, & \hat{\sigma}_i^Y &\simeq \hat{p}_i/\sqrt{s}, \\ \hat{\sigma}_i^Z &= 1 - \frac{\hat{q}_i^2 + \hat{p}_i^2 - 1}{2s}, \end{aligned} \quad (3)$$

where $s = 1/2$ for the current case, and keep only terms in the Hamiltonian (1) which are quadratic in the spin-waves modes $(\tilde{q}_k, \tilde{p}_k)$, i.e. the Fourier transform of (q_i, p_i) .

The evolution of the spherical angles is determined by the self-consistent equations $S^X(t) = S^Y(t) = 0$, which in our analysis read as

$$\begin{cases} s\dot{\phi} = p\lambda(\sin\theta)^{p-2}(\cos\phi)^p \cos\theta\{1 - (p-1)\epsilon(t)\} - g \\ \quad - 2\delta^{qq}(t) \cos\theta \cos^2\phi + 2\delta^{qp}(t) \sin\phi \cos\phi \\ s\dot{\theta} = p\lambda(\sin\theta \cos\phi)^{p-1} \sin\phi\{1 - (p-1)\epsilon(t)\} + \\ \quad - 2\delta^{pp}(t) \sin\theta \sin\phi \cos\phi \\ \quad + 2\delta^{qp}(t) \sin\theta \cos\theta \cos^2\phi \end{cases} \quad (4)$$

where we defined the quantum feedback $\delta^{\alpha\beta}(t) \equiv \sum_{k \neq 0} \Delta_k^{\alpha\beta} \cos k/(Ns)$ with $\alpha, \beta \in \{p, q\}$ and the corre-

sponding spin-wave correlation functions

$$\begin{aligned} \Delta_k^{qq}(t) &\equiv \langle \tilde{q}_k(t) \tilde{q}_{-k}(t) \rangle, & \Delta_k^{pp}(t) &\equiv \langle \tilde{p}_k(t) \tilde{p}_{-k}(t) \rangle, \\ \Delta_k^{qp}(t) &\equiv \langle \tilde{q}_k(t) \tilde{p}_{-k}(t) + \tilde{p}_k(t) \tilde{q}_{-k}(t) \rangle / 2, \end{aligned} \quad (5)$$

whose evolution is ruled by another set of differential equations, coupled to $\theta(t)$ and $\phi(t)$ (see Sup. Mat. [30, 43]). The validity of this gaussian approximation is controlled by the spin-wave density

$$\epsilon(t) = \frac{1}{Ns} \sum_{k \neq 0} \frac{\Delta_k^{qq}(t) + \Delta_k^{pp}(t) - 1}{2} \quad (6)$$

which has to be small. Before the quench, we prepare the system in a fully polarized state along the x -direction, so that $\theta(0) = 0$ and $\phi(0) = 0$, and assume that no spin-wave mode is excited, by imposing that $\Delta_k^{qq}(0) = \Delta_k^{pp}(0) = 1/2$ and $\Delta_k^{qp}(0) = 0$.

The presence of spin-waves opens a channel for internal dissipation: the zero-mode is damped by the emission of spin waves, an effect that is behind the disruption of the dynamical critical point for $p = 2$ and the emergence of a chaotic crossover phase instead. It is natural to ask

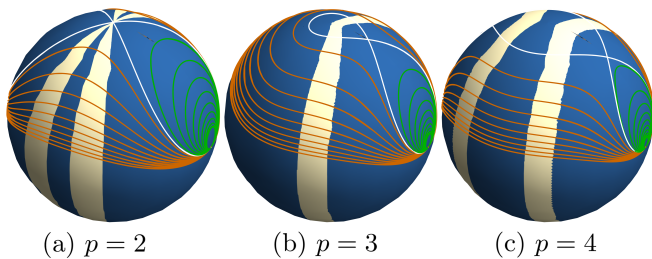


FIG. 3. Spherical plot of $\text{Re}[\nu_{k=0}(\theta, \phi)]$ of the eigenvalue with largest real part of the matrix determining the time-growth of spin-waves modes (see Supplementary Material), for $p = 2, 3, 4$. We also show on the sphere the mean-field trajectories (see also Fig.1). A nonzero value (beige) is retrieved only in a region close with a significant overlap with the paramagnetic pole ($S^z = 1$). In this area are concentrated most of the spin-wave emissions and the resulting damping of the magnetization.

if spin-wave emission is going to have the same effect in the first order case $p > 2$. To understand the effects of fluctuation on the mean-field dynamical transition, we integrate equations Eq.(4) simultaneously with the ones describing the evolution of the correlators $\Delta_k^{\alpha\beta}(t)$. We reconstruct the non-equilibrium phase diagram for $\overline{S^x}$ as a function of several values of the couplings g and J , verifying that at each time the spin-wave density $\epsilon(t)$ stays small.

If spin waves were emitted at a constant rate in time, the damped zero-mode dynamics in a paramagnetic phase would lead to localization of the latter in one the minima of the energy landscape on the Bloch sphere, either the paramagnetic minimum or one of the ferromagnetic minima (a single one for $p \geq 3$ odd or a pair for $p \geq 3$ even). The phase diagram obtained for $p = 3$ in Fig. 2-(a) shows that this is not the case: the dynamical ferromagnetic phase is of course robust against fluctuations, while the dynamical one with trajectories encompassing both minima (orange trajectories in Fig. 1-(a)) is not and for sufficiently large short-range perturbation the initial chaotic region present close to g_{dyn} becomes a fully *dynamical paramagnetic phase*. This indicates that in this case localization in the paramagnetic minimum happens predominantly. A similar phenomenon is observed also for $p \geq 4$ even, where the collective spin $\vec{S}(t)$, initially oscillating in the mean-field paramagnetic region, suddenly falls into the well around $S^x = 0$, when J is sufficiently strong. Unfortunately, this discontinuity in the time-evolution can not be appreciated by looking at the average $\overline{S^x}$, which vanishes both before and after the fall [43]. We instead examine the behaviour of the time-averaged fluctuations [35], defined as

$$\overline{(\delta S^x)^2} = \lim_{T \rightarrow \infty} \frac{1}{T} \int_0^T dt (S^x(t) - \overline{S^x})^2 \quad (7)$$

which has very different values for oscillations which are

localized in a single well or explore the whole energy landscape, as it can be clearly observed from Fig. 2-(b).

These results are very different from the ones found in [30] in the case of $p = 2$, where the same fluctuations lead to the rise of dynamical chaos. This curious discrepancy has to be imputed entirely to the stability properties of the stationary point $S^x = 0$. Indeed, the spin-wave emission is determined by the linear differential equations [43] ruling the evolution of the correlators Eq.(5), and in particular by the corresponding eigenvalue with greatest real part $\text{Re}[\nu_{k=0}(\theta, \phi)]$, which depends parametrically on the angles θ and ϕ (see [43] for a more detailed discussion). In Fig. 3, we show that this takes nonzero values only in some region around the plane $S^x = 0$, where spin-wave emission and dissipation are thus concentrated. For $p = 2$, the emission is stronger close to an unstable stationary point and the drag due to the fluctuation induces dynamical chaos, while for $p > 2$ the unstable maximum becomes a stable minimum and the collective spin moves on stable orbits around it after being damped. In summary, the nature of the dynamical quantum phases, as well the order of the transition, are unveiled by the classification of the stationary point in $S^x = 0$, which exhibits a bifurcation when moving from $p > 2$ to $p = 2$, analogous to the ones occurring in classical dynamical systems [44].

In conclusion, in this work we have studied the the post-quench dynamics of a fully-connected p -spin model ($p > 2$) perturbed by short-ranged interactions, controlled by the coupling J , generalizing to arbitrary values of p the system studied in previous work [27, 29, 30]. In the limit of $J = 0$, the dynamics is equivalent to the one of a particle in a classical energy landscape: a DQPT emerges, driven by the transverse field g , whose order depends on the parity of p which determines the shape of the potential: second order for odd p and first order for even p . The nature of this transition is modified by the presence of a short-range perturbation, treated in the framework of the non-equilibrium spin-wave theory. The latter generates an effective drag on the dynamics which is maximal in a region close to the paramagnetic pole $S^z = 1$: this changes the nature of the dynamical phases that appear on the phase diagram, reestablishing a first order transition for p odd while displaying a subtle transition detected in the order parameter fluctuations for p even. In fact, the analysis discussed here can be straightforwardly generalized to a wider class of fully-connected spin models with generic integrability breaking terms: the profile of the energy landscape and the regions where the spin-wave are emitted are the only two ingredients which fully determine the features of the non-equilibrium phase diagram.

Acknowledgements — We thank A. Leroze for interesting discussions.

-
- [1] A. Polkovnikov, K. Sengupta, A. Silva, and M. Vengalattore, Colloquium: Nonequilibrium dynamics of closed interacting quantum systems, *Reviews of Modern Physics* **83**, 863 (2011).
- [2] D. Rossini, A. Silva, G. Mussardo, and G. E. Santoro, Effective thermal dynamics following a quantum quench in a spin chain, *Phys. Rev. Lett.* **102**, 127204 (2009).
- [3] P. Calabrese, F. H. L. Essler, and M. Fagotti, Quantum quench in the transverse-field ising chain, *Phys. Rev. Lett.* **106**, 227203 (2011).
- [4] A. Maraga, P. Smacchia, M. Fabrizio, and A. Silva, Nonadiabatic stationary behavior in a driven low-dimensional gapped system, *Phys. Rev. B* **90**, 041111 (2014).
- [5] A. Polkovnikov, Universal adiabatic dynamics in the vicinity of a quantum critical point, *Phys. Rev. B* **72**, 161201 (2005).
- [6] W. H. Zurek, U. Dorner, and P. Zoller, Dynamics of a quantum phase transition, *Phys. Rev. Lett.* **95**, 105701 (2005).
- [7] J. Dziarmaga, Dynamics of a quantum phase transition: Exact solution of the quantum ising model, *Phys. Rev. Lett.* **95**, 245701 (2005).
- [8] R. W. Cherng and L. S. Levitov, Entropy and correlation functions of a driven quantum spin chain, *Phys. Rev. A* **73**, 043614 (2006).
- [9] S. Braun, M. Friesdorf, S. S. Hodgman, M. Schreiber, J. P. Ronzheimer, A. Riera, M. del Rey, I. Bloch, J. Eisert, and U. Schneider, Emergence of coherence and the dynamics of quantum phase transitions, *Proceedings of the National Academy of Sciences* **112**, 3641 (2015), <https://www.pnas.org/content/112/12/3641.full.pdf>.
- [10] M. Anquez, B. A. Robbins, H. M. Bharath, M. Boguslawski, T. M. Hoang, and M. S. Chapman, Quantum kibble-zurek mechanism in a spin-1 bose-einstein condensate, *Phys. Rev. Lett.* **116**, 155301 (2016).
- [11] L. W. Clark, L. Feng, and C. Chin, Universal space-time scaling symmetry in the dynamics of bosons across a quantum phase transition, *Science* **354**, 606 (2016), <https://science.sciencemag.org/content/354/6312/606.full.pdf>.
- [12] B. M. Anderson, L. W. Clark, J. Crawford, A. Glatz, I. S. Aranson, P. Scherpelz, L. Feng, C. Chin, and K. Levin, Direct lattice shaking of bose condensates: Finite momentum superfluids, *Phys. Rev. Lett.* **118**, 220401 (2017).
- [13] S. Kang, S. W. Seo, J. H. Kim, and Y. Shin, Emergence and scaling of spin turbulence in quenched antiferromagnetic spinor bose-einstein condensates, *Phys. Rev. A* **95**, 053638 (2017).
- [14] A. Keesling, A. Omran, H. Levine, H. Bernien, H. Pichler, S. Choi, R. Samajdar, S. Schwartz, P. Silvi, S. Sachdev, P. Zoller, M. Endres, M. Greiner, V. Vuletić, and M. D. Lukin, Quantum kibble-zurek mechanism and critical dynamics on a programmable rydberg simulator, *Nature* **568**, 207 (2019).
- [15] J.-M. Cui, F. J. Gómez-Ruiz, Y.-F. Huang, C.-F. Li, G.-C. Guo, and A. del Campo, Experimentally testing quantum critical dynamics beyond the kibble-zurek mechanism, *Communications Physics* **3**, 44 (2020).
- [16] T. Świsłocki, E. Witkowska, J. Dziarmaga, and M. Matuszewski, Double universality of a quantum phase transition in spinor condensates: Modification of the kibble-zurek mechanism by a conservation law, *Phys. Rev. Lett.* **110**, 045303 (2013).
- [17] I. B. Coulamy, A. Saguia, and M. S. Sarandy, Dynamics of the quantum search and quench-induced first-order phase transitions, *Phys. Rev. E* **95**, 022127 (2017).
- [18] K. Shimizu, T. Hirano, J. Park, Y. Kuno, and I. Ichinose, Out-of-equilibrium dynamics of multiple second-order quantum phase transitions in an extended bose-hubbard model: Superfluid, supersolid, and density wave, *Phys. Rev. A* **98**, 063603 (2018).
- [19] L. Del Re, M. Fabrizio, and E. Tosatti, Nonequilibrium and nonhomogeneous phenomena around a first-order quantum phase transition, *Phys. Rev. B* **93**, 125131 (2016).
- [20] A. Sinha, T. Chanda, and J. Dziarmaga, Nonadiabatic dynamics across a first-order quantum phase transition: Quantized bubble nucleation, *Phys. Rev. B* **103**, L220302 (2021).
- [21] G. Lagnese, F. M. Surace, M. Kormos, and P. Calabrese, False vacuum decay in quantum spin chains (2021), [arXiv:2107.10176 \[cond-mat.stat-mech\]](https://arxiv.org/abs/2107.10176).
- [22] L.-Y. Qiu, H.-Y. Liang, Y.-B. Yang, H.-X. Yang, T. Tian, Y. Xu, and L.-M. Duan, Observation of generalized kibble-zurek mechanism across a first-order quantum phase transition in a spinor condensate, *Science Advances* **6**, 10.1126/sciadv.aba7292 (2020), <https://advances.sciencemag.org/content/6/21/eaba7292.full.pdf>.
- [23] M. Heyl, A. Polkovnikov, and S. Kehrein, Dynamical quantum phase transitions in the transverse-field ising model, *Physical review letters* **110**, 135704 (2013).
- [24] M. Heyl, Dynamical quantum phase transitions: a review, *Reports on Progress in Physics* **81**, 054001 (2018).
- [25] S. A. Weidinger, M. Heyl, A. Silva, and M. Knap, Dynamical quantum phase transitions in systems with continuous symmetry breaking, *Phys. Rev. B* **96**, 134313 (2017).
- [26] B. Žunkovič, M. Heyl, M. Knap, and A. Silva, Dynamical quantum phase transitions in spin chains with long-range interactions: Merging different concepts of nonequilibrium criticality, *Phys. Rev. Lett.* **120**, 130601 (2018).
- [27] B. Sciolla and G. Biroli, Dynamical transitions and quantum quenches in mean-field models, *Journal of Statistical Mechanics: Theory and Experiment* **2011**, P11003 (2011).
- [28] P. Jurcevic, H. Shen, P. Hauke, C. Maier, T. Brydges, C. Hempel, B. P. Lanyon, M. Heyl, R. Blatt, and C. F. Roos, Direct observation of dynamical quantum phase transitions in an interacting many-body system, *Phys. Rev. Lett.* **119**, 080501 (2017).
- [29] B. Žunkovič, M. Heyl, M. Knap, and A. Silva, Dynamical quantum phase transitions in spin chains with long-range interactions: Merging different concepts of nonequilibrium criticality, *Physical Review Letters* **120**, 10.1103/physrevlett.120.130601 (2018).
- [30] A. Lerose, J. Marino, B. Žunkovič, A. Gambassi, and A. Silva, Chaotic dynamical ferromagnetic phase induced by nonequilibrium quantum fluctuations, *Phys. Rev. Lett.* **120**, 130603 (2018).
- [31] A. Lerose, B. Žunkovič, J. Marino, A. Gambassi, and A. Silva, Impact of nonequilibrium fluctuations on prethermal dynamical phase transitions in long-range interacting spin chains, *Physical Review B* **99**, 10.1103/physrevb.99.045128 (2019).
- [32] G. Piccitto, B. Žunkovič, and A. Silva, Dynamical phase

- diagram of a quantum ising chain with long-range interactions, *Phys. Rev. B* **100**, 180402 (2019).
- [33] G. Piccitto and A. Silva, Crossover from fast to slow dynamics in a long range interacting ising chain, *Journal of Statistical Mechanics: Theory and Experiment* **2019**, 094017 (2019).
- [34] E. Canovi, P. Werner, and M. Eckstein, First-order dynamical phase transitions, *Phys. Rev. Lett.* **113**, 265702 (2014).
- [35] P. Wang and R. Fazio, Dissipative phase transitions in the fully connected ising model with p -spin interaction, *Physical Review A* **103**, 10.1103/physreva.103.013306 (2021).
- [36] B. Derrida, Random-energy model: Limit of a family of disordered models, *Physical Review Letters* **45**, 79 (1980).
- [37] B. Derrida, Random-energy model: An exactly solvable model of disordered systems, *Physical Review B* **24**, 2613 (1981).
- [38] T. Jörg, F. Krzakala, J. Kurchan, A. C. Maggs, and J. Pujos, Energy gaps in quantum first-order mean-field-like transitions: The problems that quantum annealing cannot solve, *EPL (Europhysics Letters)* **89**, 40004 (2010).
- [39] V. Bapst and G. Semerjian, On quantum mean-field models and their quantum annealing, *Journal of Statistical Mechanics: Theory and Experiment* **2012**, P06007 (2012).
- [40] A. Das, K. Sengupta, D. Sen, and B. K. Chakrabarti, Infinite-range ising ferromagnet in a time-dependent transverse magnetic field: Quench and ac dynamics near the quantum critical point, *Physical Review B* **74**, 10.1103/physrevb.74.144423 (2006).
- [41] A. Rückriegel, A. Kreisel, and P. Kopietz, Time-dependent spin-wave theory, *Physical Review B* **85**, 10.1103/physrevb.85.054422 (2012).
- [42] A. Auerbach, *Interacting electrons and quantum magnetism* (Springer Science & Business Media, 2012).
- [43] See Supplemental Material.
- [44] A. Vulpiani, F. Cecconi, and M. Cencini, *Chaos: from simple models to complex systems*, Vol. 17 (World Scientific, 2009).

Supplementary Material: Changing the order of a dynamical phase transition through fluctuations in a quantum p-spin model.

In this Supplementary Material we provide more details about the methods and results presented in the main text. In Section 1, we review the time-dependent spin-wave theory and derive the equations of motion Eq.(4). In Section 2, we provide some more results which give further insight on the non-equilibrium phases. Finally, in Section 3, we analyze the spin-wave emission mechanism in greater detail.

1. Review of the spin-wave analysis

In this section, we review the time-dependent spin-wave analysis, following the same path introduced in [30]. This is implemented essentially in three steps:

1. first, we express the dynamical evolution in a rotating reference frame \mathcal{R} , defined in such a way that the magnetization is always aligned with the \mathbf{Z} -axis;
2. performing an Holstein-Primakoff in \mathcal{R} , we introduce the *spin-waves*, defined as canonical coordinates representing the spatial fluctuation of the collective spin on various length scales;
3. we derive a set of coupled equations describing the evolution of the collective spin, which is obtained requiring that the frame \mathcal{R} is aligned with the collective spin at any time, and of the spin-wave correlators, which act as a quantum feedback on the former.

Rotating frame of reference coordinates

We approach the problem by rewriting down the full Hamiltonian studied in the main text in a time-dependent, rotating frame of reference, generalizing our calculations to generic spin s . Assuming periodic boundary conditions, the Hamiltonian can be written as

$$\hat{H} = -\frac{\lambda}{N^{p-1}} (\tilde{\sigma}_0^x)^p - g\tilde{\sigma}_0^z - \frac{J}{N} \sum_{k \neq 0} \cos k \tilde{\sigma}_k^x \tilde{\sigma}_{-k}^x, \quad (8)$$

where the Fourier modes are defined as $\tilde{\sigma}_k^\alpha = \sum_{j=1}^N e^{-ikj} \hat{\sigma}_j^\alpha$ (with $\hat{\sigma}_j^\alpha = \hat{s}_j^\alpha/s$ being the rescaled spin operator on the lattice site j) and $k = 2\pi n/N$ for $n = 0, \dots, N-1$, N being the system size.

The reference frame \mathcal{R} is identified by the time-dependent Cartesian vector basis $\{\mathbf{X}(t), \mathbf{Y}(t), \mathbf{Z}(t)\}$, whose components in the original frame $\{\mathbf{x}, \mathbf{y}, \mathbf{z}\}$ read as

$$\mathbf{X} = \begin{pmatrix} \cos \theta(t) \cos \phi(t) \\ \cos \theta(t) \sin \phi(t) \\ -\sin \theta(t) \end{pmatrix}; \quad \mathbf{Y} = \begin{pmatrix} -\sin \phi(t) \\ \cos \phi(t) \\ 0 \end{pmatrix}; \quad \mathbf{Z} = \begin{pmatrix} \sin \theta \cos \phi(t) \\ \sin \theta \sin \phi(t) \\ \cos \theta(t) \end{pmatrix}$$

and where the spherical angles $\theta(t)$ and $\phi(t)$ are defined so that the average magnetization $\vec{S}(t) = \langle \sum_j \vec{\sigma}_j(t) \rangle / N$ is always aligned with $\mathbf{Z}(t)$. This change of frame is implemented on the spin Hilbert space by the time-dependent unitary rotation

$$V(\theta(t), \phi(t)) = \exp(-is\phi(t) \sum_i \sigma_i^z) \exp(-is\theta(t) \sum_i \sigma_i^y)$$

so that the spin operators transform accordingly :

$$V \hat{\sigma}_j^x V^\dagger = \mathbf{X} \cdot \vec{\sigma}_j \equiv \hat{\sigma}_j^X, \quad V \hat{\sigma}_j^y V^\dagger = \mathbf{Y} \cdot \vec{\sigma}_j \equiv \hat{\sigma}_j^Y, \quad V \hat{\sigma}_j^z V^\dagger = \mathbf{Z} \cdot \vec{\sigma}_j \equiv \hat{\sigma}_j^Z, \quad (9)$$

In this new frame, the Heisenberg equation of motion can be written as

$$\frac{d}{dt} \hat{\sigma}_j^\alpha = -i[\hat{\sigma}_j^\alpha, \tilde{H}] \quad (10)$$

where the modified Hamiltonian

$$\tilde{H} = H + iV\dot{V}^\dagger \quad (11)$$

includes an additional term $iV\dot{V}^\dagger = -s\vec{\omega}(t) \cdot \sum_j \vec{\sigma}_j$, where $\vec{\omega}(t) = (-\sin \theta \dot{\phi}, -\dot{\theta}, \cos \theta \dot{\phi})$, playing the same role of apparent forces in classical mechanics. In the rotating frame \mathcal{R} , \tilde{H} has the following form:

$$\begin{aligned} \frac{\tilde{H}}{N} = & -g \left[(\mathbf{X} \cdot \mathbf{z}) \frac{\tilde{\sigma}_0^X}{N} + (\mathbf{Y} \cdot \mathbf{z}) \frac{\tilde{\sigma}_0^Y}{N} + (\mathbf{Z} \cdot \mathbf{z}) \frac{\tilde{\sigma}_0^Z}{N} \right] - \lambda \left[(\mathbf{X} \cdot \mathbf{x}) \frac{\tilde{\sigma}_0^X}{N} + (\mathbf{Y} \cdot \mathbf{x}) \frac{\tilde{\sigma}_0^Y}{N} + (\mathbf{Z} \cdot \mathbf{x}) \frac{\tilde{\sigma}_0^Z}{N} \right]^p \\ & - J \sum_{k \neq 0} \cos k \left[(\mathbf{X} \cdot \mathbf{x}) \frac{\tilde{\sigma}_k^X}{N} + (\mathbf{Y} \cdot \mathbf{x}) \frac{\tilde{\sigma}_k^Y}{N} + (\mathbf{Z} \cdot \mathbf{x}) \frac{\tilde{\sigma}_k^Z}{N} \right] \left[(\mathbf{X} \cdot \mathbf{x}) \frac{\tilde{\sigma}_{-k}^X}{N} + (\mathbf{Y} \cdot \mathbf{x}) \frac{\tilde{\sigma}_{-k}^Y}{N} + (\mathbf{Z} \cdot \mathbf{x}) \frac{\tilde{\sigma}_{-k}^Z}{N} \right] \\ & + \sin \theta s \dot{\phi} \frac{\tilde{\sigma}_0^X}{N} - s \dot{\theta} \frac{\tilde{\sigma}_0^Y}{N} - \cos \theta s \dot{\phi} \frac{\tilde{\sigma}_0^Z}{N}, \end{aligned} \quad (12)$$

Once the equations of motion are formally written in the new frame, $\theta(t)$ and $\phi(t)$ are obtained self-consistently by imposing that

$$\begin{cases} \langle \tilde{\sigma}_0^X(t) \rangle = 0 \\ \langle \tilde{\sigma}_0^Y(t) \rangle = 0 \end{cases} \quad (13)$$

Holstein-Primakoff transformation

The main idea at the basis of time-dependent spin-wave theory is that in the new frame, as long as the spatial fluctuations induced by the short-range coupling J are weak enough, these act as a small perturbation on top of a "classical" average collective spin. In this case, we can rewrite the spin operators via the well known Holstein-Primakoff transformation [42]

$$\begin{cases} \hat{\sigma}_j^X \sim \hat{q}_j / \sqrt{s} + O(1/s^{3/2}) \\ \hat{\sigma}_j^Y \sim \hat{p}_j / \sqrt{s} + O(1/s^{3/2}) \\ \hat{\sigma}_j^Z = 1 - \frac{\hat{q}_j^2 + \hat{p}_j^2 - 1}{2s} \end{cases} \quad (14)$$

expanded in powers of $1/\sqrt{s}$ and truncated to the leading order. In terms of the Fourier space variables $\tilde{q}_k = \sum_r e^{-ikr} \hat{q}_r/\sqrt{N}$ and $\tilde{p}_k = \sum_r e^{-ikr} \hat{p}_r/\sqrt{N}$, can also be expressed as [42]:

$$\begin{cases} \frac{\tilde{\sigma}_k^x}{N} \sim \tilde{q}_k/\sqrt{Ns} + O(1/s^{3/2}) \\ \frac{\tilde{\sigma}_k^y}{N} \sim \tilde{p}_k/\sqrt{Ns} + O(1/s^{3/2}) \\ \frac{\tilde{\sigma}_k^z}{N} = 1 - \frac{1}{2Ns} \sum_{k'} (\tilde{q}_{k'}\tilde{q}_{k-k'} + \tilde{p}_{k'}\tilde{p}_{k-k'} - \delta_{k,0}) \end{cases} \quad (15)$$

This approximation is exact both in the limit of large spin $s \rightarrow \infty$, or, as stated before, when the spin-wave degree of excitation is kept small throughout the dynamics, in a sense which is made clear below.

The whole sense of our approximation is that we are expanding on-site fluctuations of the spin along the \mathbf{Z} -axis in terms of harmonic excitations, defined in terms of ladder operators $\hat{a}_j = (\hat{q}_j + i\hat{p}_j)/\sqrt{2}$ and his conjugate \hat{a}_j^\dagger : their fourier Transform $\tilde{a}_k = \sum_j e^{-ikj} \hat{a}_j/\sqrt{N}$ represent the spin-wave excitations which destroy coherence in the system. This is valid as long as the corresponding spin-wave density is small, i.e.

$$\epsilon(t) \equiv \frac{1}{Ns} \sum_{k \neq 0} \langle \tilde{a}_k^\dagger \tilde{a}_k(t) \rangle = \frac{1}{Ns} \sum_{k \neq 0} \left\langle \frac{\tilde{q}_k(t)\tilde{q}_{-k}(t) + \tilde{p}_k(t)\tilde{p}_{-k}(t) - 1}{2} \right\rangle \ll 1 \quad (16)$$

This condition sets a limit on the validity of the time-dependent spin-wave theory.

Equations of motion for weak spin-wave excitation

As long as the occupation of the $k \neq 0$ momentum modes is small, one can assume that dynamics is dominated by the lowest nontrivial order in the spin-wave degrees of freedom, that is by a Gaussian approximation, in our case. This means that, plugging the new canonical variables into the Eq.(12), we can replace the Hamiltonian \tilde{H} with its expansion in the operators $\{(\tilde{q}_k, \tilde{p}_k)\}$ to the quadratic order. Then we determine explicitly the orientation of the time-dependent frame \mathcal{R} , through the equations (13). Within the Gaussian approximation, these read as

$$\begin{cases} s\dot{\phi} = p\lambda(\sin\theta)^{p-2}(\cos\phi)^p \cos\theta \{1 - (p-1)\epsilon(t)\} - g - 2\delta^{qq}(t) \cos\theta \cos^2\phi + 2\delta^{qp}(t) \sin\phi \cos\phi \\ s\dot{\theta} = p\lambda(\sin\theta \cos\phi)^{p-1} \sin\phi \{1 - (p-1)\epsilon(t)\} - 2\delta^{pp}(t) \sin\theta \sin\phi \cos\phi + 2\delta^{qp}(t) \sin\theta \cos\theta \cos^2\phi \end{cases} \quad (17)$$

with the quantum feedback being $\delta^{\alpha\beta}(t) \equiv \sum_{k \neq 0} \Delta_k^{\alpha\beta} \cos k/(Ns)$ for $\alpha, \beta \in \{p, q\}$, as stated in the main text.

We see that, within time-dependent spin-wave theory, the motion of the collective spin is coupled to the one of the correlation functions

$$\begin{cases} \Delta_k^{qq}(t) = \langle \tilde{q}_{-k}(t)\tilde{q}_k(t) \rangle \\ \Delta_k^{qp}(t) = \langle \frac{\tilde{q}_{-k}(t)\tilde{p}_k(t) + \tilde{p}_{-k}(t)\tilde{q}_k(t)}{2} \rangle \\ \Delta_k^{pp}(t) = \langle \tilde{p}_{-k}(t)\tilde{p}_k(t) \rangle \end{cases} \quad (18)$$

where all the averages are performed with respect to the initial state. The evolution of the variables $\{\Delta_k^{\alpha\beta}(t)\}$ is straightforwardly determined by the Heisenberg equations of motion for the canonical variables $(\tilde{q}_k, \tilde{p}_k)$:

$$\begin{cases} s \frac{d\tilde{q}_k}{dt} = (p\lambda(\sin\theta)^{p-2} \cos^p\phi - 2J \cos k \sin^2\phi) \tilde{p}_k + 2J \cos k \cos\theta \sin\phi \cos\phi \tilde{q}_k \\ s \frac{d\tilde{p}_k}{dt} = -(\lambda(\sin\theta)^{p-2} \cos^p\phi - 2J \cos k \cos^2\phi \cos^2\theta) \tilde{q}_k - (2J \cos k \cos\theta \sin\phi \cos\phi) \tilde{p}_k \end{cases} \quad (19)$$

and reads as

$$\begin{cases} s \frac{d}{dt} \Delta_k^{qq} = (4J \cos k \cos\theta \sin\phi \cos\phi) \Delta_k^{qq} + \{2p\lambda(\sin\theta)^{p-2} \cos^p\phi - 4J \cos k \sin^2\phi\} \Delta_k^{qp} \\ s \frac{d}{dt} \Delta_k^{qp} = -\{p\lambda(\sin\theta)^{p-2} \cos^p\phi - 2J \cos k \cos^2\phi \cos^2\theta\} \Delta_k^{qq} \\ \quad + \{p\lambda(\sin\theta)^{p-2} \cos^p\phi - 2J \cos k \sin^2\phi\} \Delta_k^{pp} \\ s \frac{d}{dt} \Delta_k^{pp} = -\{2p\lambda(\sin\theta)^{p-2} \cos^p\phi - 4J \cos k \cos^2\phi \cos^2\theta\} \Delta_k^{qp} \\ \quad - (4J \cos k \cos\theta \sin\phi \cos\phi) \Delta_k^{pp} \end{cases} \quad (20)$$

From equations Eq.(20), it is also possible to prove that, for any fixed momentum k , the time-evolution of the three spin-wave correlators is completely specified by two of them, as they have to satisfy the constraint

$$(\Delta_k^{qp}(t))^2 = \Delta_k^{qq}(t)\Delta_k^{pp}(t) - \frac{1}{4}. \quad (21)$$

at any time t . The final result is that, within the framework of time-dependent spin-wave theory, the dynamics of the average magnetization $\vec{S}(t)$ is coupled with that of the spin-wave correlation functions $\Delta^{\alpha\beta}(t)$, which also determine the spin-wave density

$$\epsilon(t) = \frac{1}{N_S} \sum_{k \neq 0} \frac{\Delta_k^{qq}(t) + \Delta_k^{pp}(t) - 1}{2} \quad (22)$$

Integrating simultaneously the system of equations (17) and (20) and checking that $\epsilon(t) \ll 1$, one obtains the non-equilibrium dynamics of $\langle \vec{S}(t) \rangle$, coupled to spin-wave fluctuations. The initial conditions are determined by the initial state $|\psi_0\rangle$. The case we studied is the one of a quench in the Hamiltonian (1), with pre-quenches values given by $g = g_0$ and $J = 0$, which correspond to

$$\begin{aligned} \{\sin \theta(t=0)\}^{p-2} \cos \theta(t=0) &= g_0/(\lambda p), & \phi(t=0) &= 0, \\ \Delta_k^{qq}(t=0) = \Delta_k^{pp}(t=0) &= 1/2, & \text{and } \Delta_k^{qp}(t=0) &= 0, \end{aligned} \quad (23)$$

for every $k \neq 0$. This also imply that $\epsilon(t=0) = 0$, as the initial ground state $|\psi_0\rangle = |\rightarrow \cdots \rightarrow\rangle$ is perfectly coherent, with the spin on each lattice site point in the direction of the ferromagnetic minimum of \hat{H} .

In the fully-connected limit $J \rightarrow 0$ the evolution of the collective spin decouples from the fluctuations, and the equations (17) are identical to the ones predicted by the effective classical theory described in Ref. [27]. In this case, the spin-wave correlators still have a nontrivial dynamics, but the spin-wave density is conserved and always vanishes.

2. Non-equilibrium dynamics for $p \geq 4$ even

As outlined in the main text, for $p \geq 4$ even the localization induced by the spin-wave emission can not be seen immediately looking at the phase diagram for the time-averaged longitudinal magnetization $\overline{S^x}$.

Indeed, while Fig.4 shows the stability of the dynamical ferromagnetic phase, having always $\overline{S^x} > 0$, it is not clear

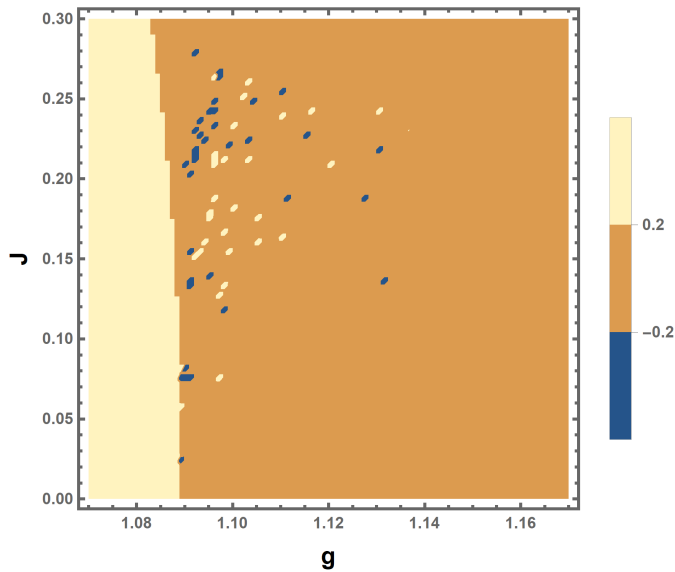


FIG. 4. Non-equilibrium phase diagram for the time-averaged magnetization $\overline{S^x}$ and for $p = 4$. Below the mean-field critical point $g = g_{dyn}$, the magnetization is always confined in the ferromagnetic region, while for $g > g_{dyn}$ $\overline{S^x}$ vanishes (except in some isolated chaotic spots), meaning that the dynamical trajectories either surround symmetrically all the three minima of the landscape or are localized in a paramagnetic well.

what happens above the mean-field critical point $g > g_{dyn}$, where the vanishing longitudinal magnetization may imply that the mean-field trajectories surrounding the three minima are stable or that the system localizes in the paramagnetic well at large times. The analysis of the time-averaged fluctuations $(\overline{\delta S^x})^2$, reported in Fig.2-(b) of the main text, clarifies that this stability persists up to some threshold in J , beyond which the magnetization falls into the paramagnetic well and performs smaller oscillations around the average $\overline{S^x} = 0$.

This phenomenon becomes even more transparent in Fig. 5 where the trajectories surrounding both the three minima fall into the paramagnetic well for large times, if the coupling J is above a certain threshold.

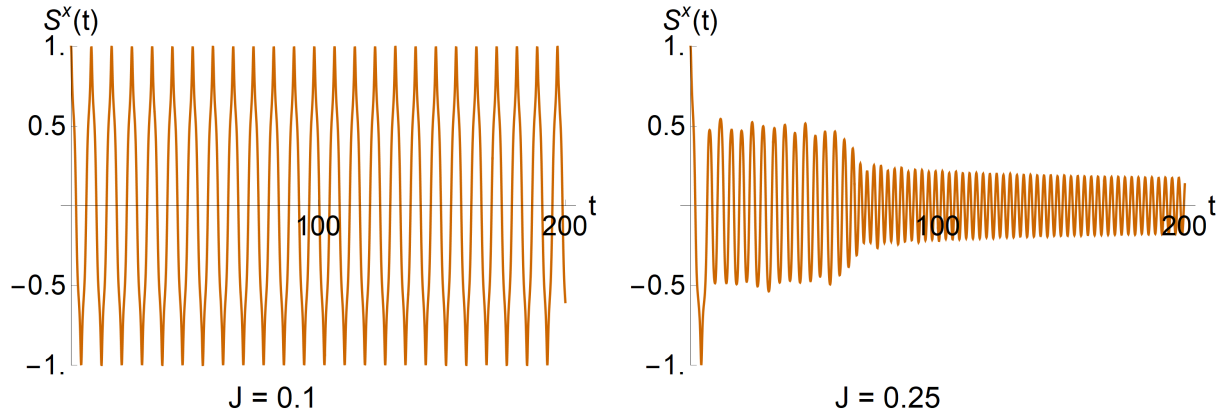


FIG. 5. Dynamics of the longitudinal magnetization $S^x(t)$ in the energy landscape described by the Hamiltonian (1) for $p = 4$, for fixed $\lambda = 1$ and $g = 1.1$, corresponding to the mean-field dynamical phase. For $J = 0.1$ the mean-field phase is stable, while for $J = 0.2$ it is not, as the collective spin falls into the paramagnetic well at large times.

3. The spin-wave emission mechanism

In this section, we explore in a more detailed way the physical mechanism behind the spin-wave emission, which leads to the localization of the magnetization $\vec{S}(t)$ at long times, as described in the main text.

The main idea is that, due to the linearity of Eq. (20), proliferation of the spin-waves is ruled by the eigenvalues of the coefficient matrix of the right-hand sides and, in particular, by their real part. Keeping the spherical angles θ and ϕ as fixed as external parameter, a straightforward diagonalization shows that, for every value of $k \neq 0$, the eigenvalues are in the form of $\{\nu_k(\theta, \phi), 0, -\nu_k(\theta, \phi)\}$ where

$$\text{Re}[\nu_k(\theta, \phi)] = 4\sqrt{p(\sin\theta)^{p-2} \cos^p(\phi) (2J \cos(k) (\cos^2(\theta) \cos^2(\phi) + \sin^2(\phi)) - p(\sin\theta)^{p-2} \cos^p(\phi))} \quad (24)$$

To get an idea of the behaviour of these function, we plotted $\text{Re}[\nu_{k=0}(\theta, \phi)]$ on the Bloch sphere in Fig. 3 of the main text and seen that it is maximised exactly for values of θ and ϕ close to the plane $S^x = 0$, so we identified it as the responsible for the localization of the system into the paramagnetic well for $p > 2$ and strong enough J . To further confirm this intuition, we also analyse a specific example of trajectory for $p = 4$, in Fig. 6: there is evident how the spin-wave density is maximised in proximity of the minimum in $S^x = 0$, and how this grows steeply when the system localizes in the paramagnetic well.

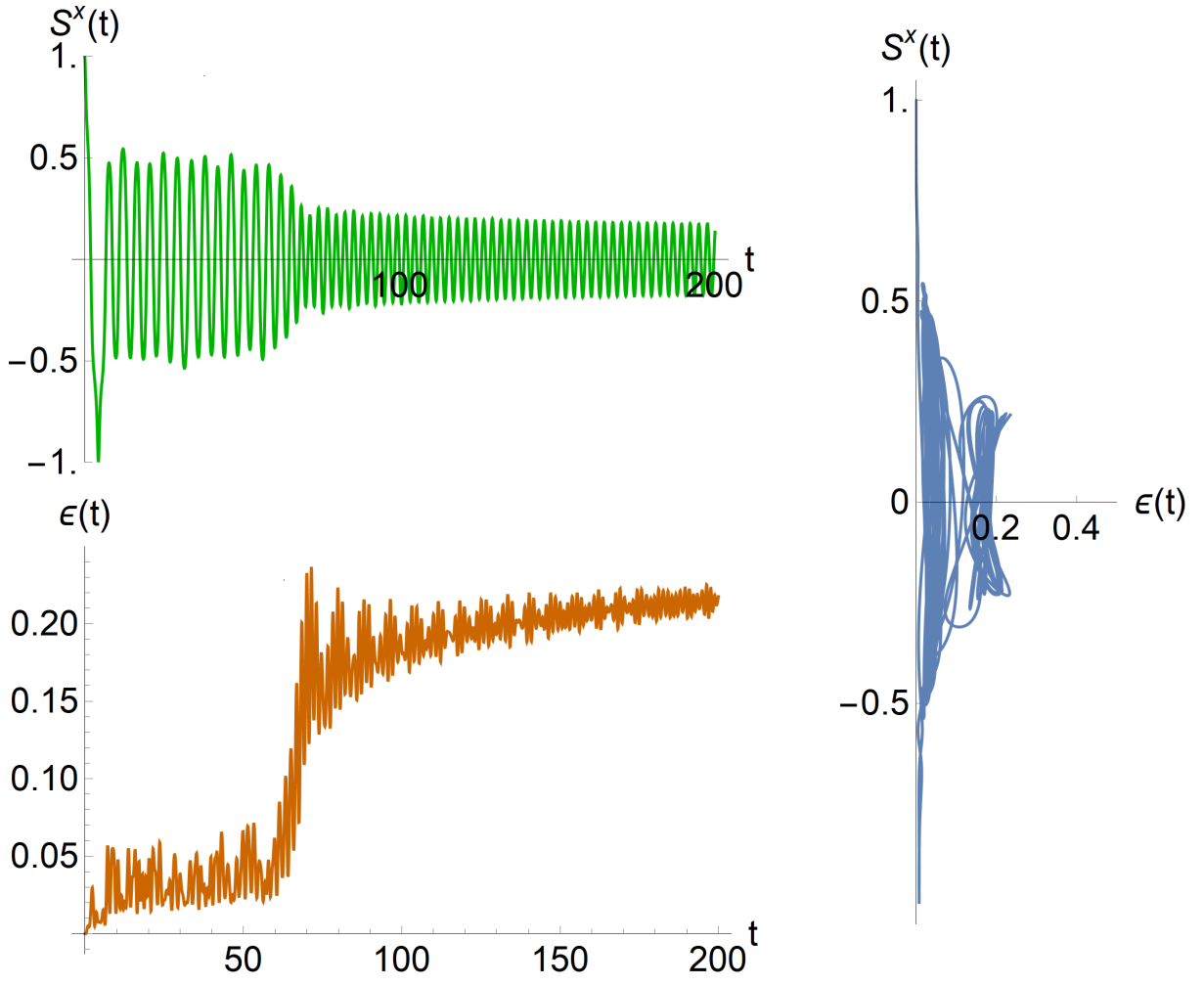


FIG. 6. **(Left)** dynamical contribution of the longitudinal magnetization $S^x(t) = 0$, compared also with the relative spin-wave density $\epsilon(t)$. When $S^x(t) = 0$ falls into the paramagnetic sector for long times, the density $\epsilon(t)$ exhibit a steep growth. Here we set the simulation parameters to $p = 4$, $g = 1.1$ and $J = 0.25$ and fixed $\lambda = 1$. **(Right)** Parametric plot of the same observables $S^x(t) = 0$ and $\epsilon(t)$. It is easy to see that the spin-wave density is maximised when $S^x(t)$ is around the paramagnetic minimum.